Thermal conductance of nanostructured phononic crystals

A. N. Cleland,* D. R. Schmidt, and C. S. Yung
Department of Physics and iQUEST, University of California at Santa Barbara, Santa Barbara, California 93106
(Received 30 May 2001; published 15 October 2001)

The thermal conductance of mechanically suspended nanostructures has recently received much attention, in part due to the recent prediction and observation of the quantum limit for thermal conductance, which is observed in long, thin insulating beams at very low temperatures [D. E. Angelescu, M. C. Cross, and M. L. Roukes, Superlattices Microstruct. **23**, 673 (1998); K. Schwab, E. A. Henriksen, J. M. Norlock, and M. L. Roukes, Nature **404**, 974 (2000); I. G. C. Rego and G. Kirczenow, Phys. Rev. Lett. **81**, 232 (1998); M. P. Blencowe, Phys. Rev. B **59**, 4992 (1999)]. In this brief report, we describe a model calculation where the simple beam used to calculate quantum conductance [L. G. C. Rego and G. Kirczenow, Phys. Rev. Lett. **81**, 232 (1998)] is replaced by a beam made from an artificial one-dimensional phononic crystal. We find that at the lowest temperatures and longest thermal-phonon wavelengths, the quantum limit is recovered, while for intermediate temperatures, where the dominant phonon wavelength is of the order of the phononic-crystal repeat distance, a significant suppression of the conductance is predicted. At higher temperatures the conductance returns to that of a simple beam.

DOI: 10.1103/PhysRevB.64.172301 PACS number(s): 65.40.−b, 65.80.+n, 62.25.+g

The ability to fabricate suspended nanoscale structures that include temperature-sensitive and electronically active devices has allowed the development of highly sensitive mechanical electrometers and calorimeters, and the recent observation of the quantum of thermal conductance.[2,5–7] In bolometric- and calorimetric-detector applications, the energy sensitivity of the detector is ultimately limited by the nanostructure heat capacity $\mathcal{C}$ and the thermal conductance $\mathcal{G}$ linking the capacitance to a temperature reservoir. In general, smaller size structures yield smaller heat capacities. The thermal links, which also act as mechanical supports for the suspended structure, give increased thermal isolation with smaller cross sections and larger length-to-diameter aspect ratios. An example of a nanoscale bolometer is shown in Fig. 1. The device consists of a small block of single-crystal GaAs, suspended by four thin beams from the bulk substrate. A pair of superconductor–insulator–normal-metal (Al-I-Cu) double-tunnel junctions have been patterned on the surface of the suspended block, and act as heaters and thermometers allowing the measurement of the thermal conductance of the supports; a more complete description of this device will appear in Ref. 8.

The thermal conductance in this structure is determined by the conductance of the four thin beams supporting the central block; these comprise a 0.2-μm-thick GaAs beam with an overlying 0.05-μm-thick superconducting Al electrode. Operated well below the superconducting transition temperature, the thermal conductance is that of an electrical insulator, dominated by the thermal conductance through the delocalized phonon modes connecting thermal reservoirs at either end of the beam. The thermal conductance $\mathcal{G}$ is given by the formula[1,3,4,9]

$$\mathcal{G}=\frac{\hbar^2}{k_B T^2}\sum_n \frac{1}{2\pi}\int_0^\infty \mathcal{T}_n(\omega)\frac{\omega^2 e^{\hbar\omega/k_B T}}{(e^{\hbar\omega/k_B T}-1)^2}\,d\omega. \qquad (1)$$

Here n runs over the delocalized phonon modes in the beam, and $\mathcal{T}_n(\omega)$ is the phonon transmissivity for that mode at frequency ω; each mode has a continuum of transmitting frequencies. Most of the modes in a beam have low-frequency cutoffs similar to those for electromagnetic waves in a waveguide; a simple beam has only four modes that do not have such cutoffs, one longitudinal, one torsional, and two flexural modes. At the lowest temperatures, therefore, only these four modes can conduct energy, and if each of these modes has transmissivity $\mathcal{T}\rightarrow 1$, the thermal conductance approaches a universal quantum limit: $\mathcal{G}_Q=N(\pi^2 k_B^2/3h)T$, with $N=4$ being the number of low-frequency modes. In this low-temperature limit, the thermal conductance is independent of the beam length and cross section, and is proportional to T. This prediction for the thermal conductance has recently

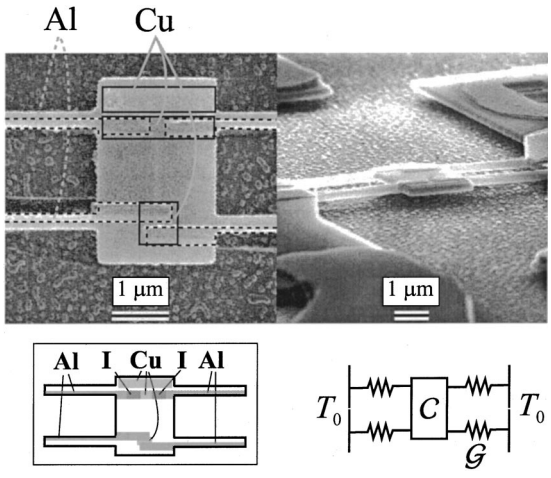

FIG. 1. Electron micrograph of a nanoscale bolometer, comprising a pair of Al-I-Cu-I-Al tunnel junctions fabricated on the surface of a $(2\times3\times0.2)$-μm^3 GaAs block, which is suspended by four $(0.2\times0.2\times4)$-μm^3 beams from the bulk substrate. Below is a sketch of the geometry including the tunnel junctions, and a highly simplified thermal model, indicating the heat capacitance $\mathcal{C}$ of the central block (dominated by that of the normal Cu metal), and thermal conductance $\mathcal{G}$ for each of the four beams.

been experimentally demonstrated by Schwab *et al.*[2]

The prediction for the low-temperature quantum limit $\mathcal{G}_Q$ appears to be quite robust. A recent calculation[9] includes the effect of surface roughness on the thermal conductance of a simple beam; the roughness causes elastic scattering between the allowed phonon modes, including scattering between forward-traveling and reverse-traveling phonons. The authors found that if the roughness has a correlation length Λ, then phonons with wavelengths much larger than or much smaller than Λ have a transmissivity approaching unity. The thermal conductance of a roughened beam is then given by the quantum limit for temperatures low enough that the characteristic phonon wavelength is larger than Λ, and returns to the dependence given by Eq. (1) for temperatures high enough that the dominant phonon wavelengths are much smaller than Λ. At temperatures between these limits, a moderate suppression of the conductance below $\mathcal{G}_Q$ is found, where the scattering is the strongest; this explains the corresponding suppression seen in the experiment[2] at intermediate temperatures.

In this paper, we investigate the thermal conductance for beams fabricated from beams made from artificial phononic crystals in the absence of scattering. Periodically modulated mechanical structures, which generate classical band structures, have been used for some time for applications in ultrasound and ultrasonic transducers;[10] a description of the current theoretical and experimental work appears in a review by Kushwaha.[11] The dispersion relation $\omega(k)$ for acoustic phonons traveling in a periodically modulated material is found to develop gaps in the transmission spectrum at wave vectors k associated with the modulation wave vector; these gaps should have an effect on the thermal conductance of a beam fabricated from such a material. We have calculated the dispersion relations for a periodically modulated, quasi-one-dimensional beam using two different acoustic models. We find that the resulting band structure, with gaps at frequencies that correspond to the phonons dominant at quite low temperatures, yields significant reductions in the thermal conductance from the quantum limit $\mathcal{G}_Q$ at moderate temperatures. However, the presence of delocalized Bloch states at the lowest phonon frequencies, below the gap, gives a thermal conductance that approaches $\mathcal{G}_Q$ at the lowest temperatures.

Our first model is for the longitudinal acoustic mode in a beam of variable cross section. x being the coordinate along the beam length, and $A(x)$ being the (position-dependent) cross-sectional area, the longitudinal displacement $u(x,t)$ satisfies the approximate one-dimensional equation[12,3]

$$\frac{1}{c_l^2}\frac{\partial^2 u}{\partial t^2}=\frac{\partial^2 u}{\partial x^2}+\frac{1}{A}\frac{\partial A}{\partial x}\frac{\partial u}{\partial x}, \tag{2}$$

where c_l is the longitudinal sound speed. We assume a periodic variation in the cross section A, of the form $\partial \ln A(x)/\partial x=\varepsilon G \sin Gx$, with amplitude ε and wave vector G (see inset to Fig. 2). The solutions to Eq. (2) can be expanded in the Bloch form with wave vector k and frequency ω,

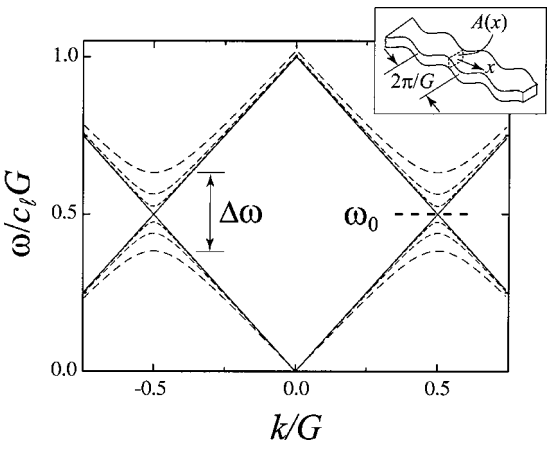

FIG. 2. Calculated dispersion relation for modulation strengths $\epsilon=0$, 0.1, 0.25, and 0.5 in the longitudinal acoustic model. The gap $\Delta\omega$ for $\varepsilon=0.5$ is indicated, as is the band-gap center frequency $\omega_0=c_lG/2$. Eleven bands were included in the calculation, the lowest two are shown here.

$$u(x,t)=\sum_{n=-\infty}^{\infty} U_n \exp[i(k+nG)x+i\omega t]. \tag{3}$$

In the limit $\varepsilon\to 0$, the terms in Eq. (2) with different n are decoupled and yield the dispersion relations $\omega^2=c_l^2(k+nG)^2$; these are drawn in Fig. 2 in a repeated-zone scheme. With nonzero ε, these terms become coupled, we numerically solve the eigenvalue equations Eq. (2).

We find that gaps $\Delta\omega$ open in the dispersion spectrum at the Brillouin-zone edges $k=\pm G/2$ corresponding to a frequency $\omega_0=c_lG/2$ in the center of the gap. In Fig. 2 we show the dispersion relations for the two lowest bands, for the unmodulated ($\varepsilon=0$) beam, and for a range of variational amplitudes ε. This structure therefore forms a one-dimensional phononic crystal, with a forbidden frequency band centered at ω_0, of magnitude $\Delta\omega/\omega_0\cong\varepsilon$.

As an example, a beam fabricated from Si with a thickness of 0.2 μm, can easily be patterned with a modulated width w varying from 0.1 to 0.5 μm with a periodicity of $2\pi/G=0.5\,\mu$m. The variational amplitude in Eq. (2) is then $\varepsilon=\frac{2}{3}$, and the corresponding bandgap is centered at $\omega_0=c_lG/2=33$ GHz. The calculation predicts a gap with bandwidth $\Delta\omega=22$ GHz, taking the sound speed $c_l=4300$ m/s.

In our second model we use a scalar phonon model of the type used by Santamore and Cross.[9] The scalar phonon displacement field $\Phi(\mathbf{r},t)$ satisfies the homogeneous wave equation with elastic modulus E and density ρ,

$$\rho\frac{\partial^2\Phi}{\partial t^2}=\boldsymbol{\nabla}\cdot(E\boldsymbol{\nabla}\Phi). \tag{4}$$

The beam is now fabricated as a composite structure with a periodic variation in the density and elastic modulus, so that $E=E(x)$ and $\rho=\rho(x)$, as sketched in Fig. 3. The beam has width w along the y axis and thickness t along z. We assume that the surfaces of the beam are stress-free, so that $\partial\Phi/\partial\hat{n}=0$ for a local surface normal $\hat{n}$ at $z=0,t$ and $y=0,w$.

The solutions to Eq. (4) are separable and have the form

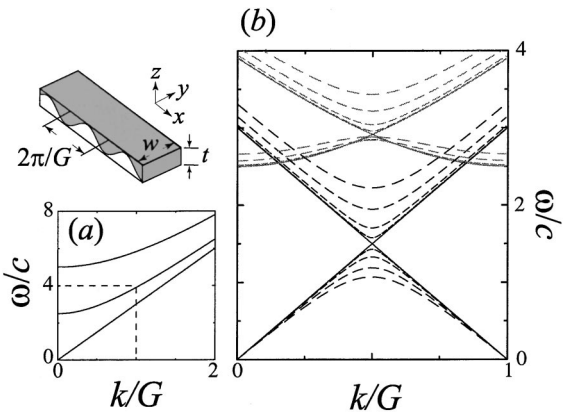

FIG. 3. (a) Dispersion relation for empty lattice, showing the three lowest modes for the scalar model, plotted in an extended-zone scheme. Dashed box shows the region plotted in detail in (b). (b) Dispersion relation including the structural modulation, plotted in the reduced-zone scheme. The calculation is for perturbation strengths $\delta=\epsilon=0.1$, 0.25, 0.5, and 0.75. Black solid and dashed lines are for the $(k_x,l,m)=(k_x,0,0)$ mode, and solid and dashed gray lines are for the $(k_x,1,0)$ mode. The geometric parameters were $w=2t$ and modulation wave vector $G=0.6\pi/t$. Inset shows the geometry for the structure.

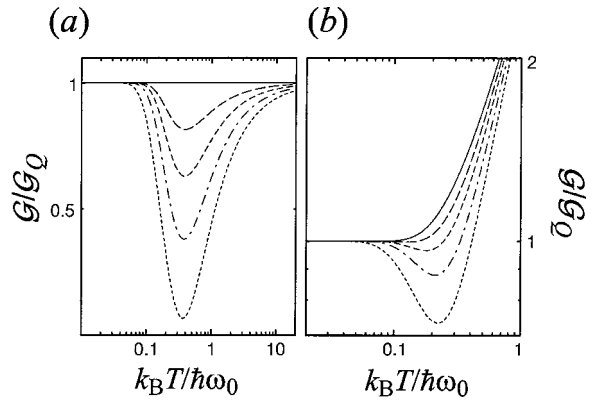

FIG. 4. (a) Calculated thermal conductance in units of the quantum of thermal conductance $\mathcal{G}_Q$ for one mode of a phononic crystal beam as a function of temperature normalized to the band-gap center ω_0. The solid line is for a simple beam showing the quantum value $\mathcal{G}/\mathcal{G}_Q=1$, and the dotted lines are for phononic crystal beams with band-gap widths $\Delta\omega/\omega_0=0.2$, 0.4, 0.6, and 1. The dotted line shows (b) Thermal conductance including the higher-order modes, for the simple beam (solid line) and for the same series of modulation widths $\Delta\omega/\omega_0$.

$$\Phi(\mathbf{r},t)=\phi(x)\cos k_{ly}\cos k_m z e^{i\omega t} \tag{5}$$

with transverse wave vectors $k_l=l\pi/w(l=0,1,2,...)$ and $k_m=m\pi/t(m=0,1,2,...)$. The function $\phi(x)$ satisfies

$$\frac{1}{\rho(x)}\left[E(x)k_l^2+E(x)k_m^2-\frac{\partial}{\partial x}E(x)\frac{\partial}{\partial x}\right]\phi=\omega^2\phi. \tag{6}$$

We assume that the elastic modulus has the spatial dependence $E(x)=E_0[1+\varepsilon\cos(Gx)]$ with a modulation amplitude ε and wave vector G; the inverse density has the same type of dependence, $1/\rho(x)=(1/\rho_0)[1+\delta\cos(Gx)]$, with amplitude δ. If ε and δ are taken to have the same sign, then an increase in elastic modulus is coupled with a decrease in density. The solutions to Eq. (6) have the same form as for our previous model with

$$\phi(x)=\sum_{n=-\infty}^{\infty}\phi_n e^{i(k_x+nG)x}. \tag{7}$$

Inserting this form into Eq. (6), we can calculate the eigenvalue solutions $\omega(k_x)$ for the modes (k_x,l,m). In the limit $\varepsilon,\delta\to 0$, the "empty-lattice" solutions $\omega^2=c_0^2(k_x^2+k_l^2+k_m^2)$ are found with wave velocity $c_0^2=E_0/\rho_0$. For nonzero ε and δ, we solve the coupled equations numerically; the solutions are plotted in Fig. 3 for the two lowest bands $(l,m)=(0,0)$ and $(l,m)=(1,0)$ as a function of longitudinal wave vector k_x. In the calculation we have retained terms of second order $\varepsilon\delta$, which mix wave vectors in band n with those in bands $n\pm 2$; dropping these does not significantly change the result shown in Fig. 3.

We again find that gaps open in the dispersion spectrum at the Brillouin-zone boundaries $k=\pm G/2$, with the magnitude for the gap between the lowest two bands approximately given by $\Delta\omega/\omega_0\cong\varepsilon$ for $\delta=\varepsilon$. If our composite structure consists of a 0.2-μm-thick beam of Si ($E=47$ GPa, $\rho=2330$ kg/m^3) combined with Pb ($E=16$ GPa, $\rho=11\,340$ kg/m^3), we have $\varepsilon\cong 0.5$ and $\delta\cong 0.65$, and we choose a periodicity $2\pi/G=0.5\,\mu$m. The calculation then yields a band center at $\omega_0=c_0G/2=14$ GHz with bandgap width $\Delta\omega=0.56\omega_0=8$ GHz.

These two approximate methods for calculating the dispersion relation of a one-dimensional phononic crystal yield rather similar results. We now consider what the implications are for the thermal transport through a beam fabricated with such a periodic structure. We assume that the beam is adiabatically coupled to thermal reservoirs at either end, using smooth, graduated increases in the cross-sectional area A to the bulk solid; we therefore avoid end-to-end phonon resonances,[3] and the acoustic mismatch from abrupt area transitions.[1,13] We calculate the temperature dependence of the thermal conductance for a single low-frequency Bloch mode with transmissivity $\mathcal{T}(\omega)$ equal to 1 for ω in the allowed bands, $0<\omega<\omega_0-\Delta\omega/2$ and $\omega>\omega_0+\Delta\omega/2$, and zero for ω in the forbidden gap region. The result of the calculation, using Eq. (1), is shown in Fig. 4(a), calculated for temperatures well below the cutoff temperature for the second mode [the mode $(k_x,1,0)$ in the scalar model, Eq. (4)]. In part (b) of that figure we display the temperature dependence including the higher-order modes.

At the lowest temperatures, such that the primary phonon frequency is much smaller than the lower band-gap edge $\omega_0-\Delta\omega/2$, the thermal conductance for the single mode is given by the quantum limit $\mathcal{G}_Q$. As the temperature is increased, the phonon distribution passes through the gap frequency ω_0, and the thermal conductance falls to a minimum at a temperature roughly given by $k_BT_{\min}\cong\hbar\omega_0/2.7$. Above this temperature, significant numbers of phonons populate the upper band; at high enough temperatures the result for a simple beam is recovered, with conduction occurring through a number of cutoff modes. This behavior is remark-

ably similar, although larger in magnitude, to that calculated for scattering due to imperfections in the surface of a simple beam, as shown by Santamore and Cross.[9] Here we can tune the amount by which the conductance is lowered at intermediate temperatures by increasing the width of the gap, and shift the point of minimum conductance by changing the crystal-repeat distance. However, at low enough temperatures the quantum of conductance will always be recovered.

For our two numerical examples cited above, the modulation of the cross-sectional width w of a Si beam from 0.1 to 0.5 μm yields a minimum in normalized thermal conductance at a temperature of 0.25 K, with a reduction by a factor of 0.7. For the composite modulated beam consisting of a modulated Si/Pb overlayer structure, the normalized conductance minimum is at 0.11 K, with a reduction factor of 0.57.

We have only considered the thermal conduction through effectively one of the four types of conducting modes in the beam. The other three modes will developed band gaps as well, at the same wave vectors $k_x = \pm G/2$, but at somewhat different center frequencies ω_0 due to the different acoustic sound speeds for these modes, and with different bandgaps $\Delta\omega$ due to the different coupling strengths. The total thermal conductance will consist of the superposed conductance associated with each mode and will therefore smear somewhat the features shown in Fig. 4. However, a significant feature should still be visible at intermediate temperatures.

In conclusion, we find that the quantum of conductance is quite robust, and for any given phononic crystal the thermal conductance at low enough temperatures will recover to the quantum limit. At moderate temperatures, however, the thermal conductance can be controllably reduced below the quantum limit, over a range of temperatures set by the fabrication parameters for the phononic crystal. This capability may prove useful in bolometric and calorimetric applications.

The authors thank Michael Geller for valuable discussions and a critical reading of the manuscript, and Robert Knobel for valuable conversations. We acknowledge the support provided by a NASA Explorer Award No. ECS-9980734, the Army Research Office under Contract No. DAAD-19-99-1-0226, and by a Research Corporation Research Innovation Award.

*Corresponding author. Email address: cleland@physics.ucsb.edu

[1] D. E. Angelescu, M. C. Cross, and M. L. Roukes, Superlattices Microstruct. **23**, 673 (1998).
[2] K. Schwab, E. A. Henriksen, J. M. Worlock, and M. L. Roukes, Nature (London) **404**, 974 (2000).
[3] L. G. C. Rego and G. Kirczenow, Phys. Rev. Lett. **81**, 232 (1998).
[4] M. P. Blencowe, Phys. Rev. B **59**, 4992 (1999).
[5] A. N. Cleland and M. L. Roukes, Nature (London) **320**, 160 (1998).
[6] M. L. Roukes, Physica B **263–264**, 1 (1999).
[7] P. Singha Deo, J. P. Pekola, and M. Manninen, Europhys. Lett. **50**, 649 (2000).
[8] C. S. Yung and A. N. Cleland (unpublished).
[9] D. H. Santamore and M. C. Cross, Phys. Rev. B **63**, 184306 (2001).
[10] M. Torres, F. R. Montero de Espinosa, and J. L. Aragón, Phys. Rev. Lett. **86**, 4282 (2001).
[11] M. S. Kushwaha, Int. J. Mod. Phys. B **10**, 977 (1996).
[12] Karl F. Graff, *Wave Motion in Elastic Solids* (Dover, New York, 1975).
[13] M. C. Cross and R. Lifshitz, cond-mat/0011501 (unpublished).